LLNL-PROC-419388

LAWRENCE
LIVERMORE
NATIONAL
LABORATORY

Experimental Evaluation of Neutron Induced Noise on Gated X-ray Framing Cameras

N. Izumi, G. Stone, C. Hagmann, C. Sorce, D. K. Bradley, M. Moran, O. L. Landen, W. Stoeffl, P. Springer, R. Tommasini, H. W. Hermann, G. A. Kyrala, V. Y. Glebov, T. C. Sangster, J. A. Koch

November 3, 2009

Inertial Fusion Sciences and Applications 2009
San Francisco, CA, United States
September 6, 2009 through September 11, 2009

This work performed under the auspices of the U.S. Department of Energy by Lawrence Livermore National Laboratory under Contract DE-AC52-07NA27344.

Experimental evaluation of neutron induced noise on gated x-ray framing cameras

N Izumi, G Stone, C Hagmann, C Sorce, D K Bradley, M Moran, O L Landen, P Springer, W Stoeffl, R Tommasini, H W Hermann[1], G A Kyrala[1], V Y Glebov[2], T C Sangster[2] , and J A Koch

Lawrence Livermore National Laboratory, Livermore, CA, USA

[1]Los Alamos National Laboratory, Los Alamos, NM, USA

[2]Laboratory for Laser Energetics, Rochester, NY, USA

izumi2@llnl.gov

Abstract. A micro-channel plate based temporally-gated x-ray camera (framing camera) is one of the most versatile diagnostic tools of inertial confinement fusion experiments; particularly for observation of the shape of x-ray self emission from compressed core of imploded capsules. However, components used in an x-ray framing camera have sensitivity to neutrons induced secondary radiations. On early low-yield capsule implosions at the National Ignition Facility (NIF), the expected neutron production is about 5×10^{14}. Therefore, the expected neutron fluence at a framing camera located ~ 150 cm from the object is 2×10^{9} neutrons/cm^{2}. To obtain gated x-ray images in such harsh neutron environments, quantitative understanding of neutron-induced backgrounds is crucial.

1. Introduction

Because of their long mean free path, 14-MeV neutrons produced by the t(d,n)α reaction penetrate x-ray shielding along the detector line of sight, causing various interactions in materials surrounding the sensitive region of the x-ray framing camera such as elastic recoil, (n,n')γ, (n,p), (n,α). These secondary ionizing radiations or visible light produced by these radiations, then stimulate the sensitive layer of the detector and induce background noise. To understand mechanisms of this neutron induced background, we have fabricated a test camera head and exposed it to strong DT neutron fluxes at the Omega laser facility.

2. Gated and time integrated components of x-ray framing camera

Fig. 1. shows a typical setup of pinhole imaging with an x-ray framing camera at the National Ignition facility. A pinhole array is located typically 8~20 cm from the capsule. The x-ray image is projected on to a micro-channel plate (MCP) surface (~150 cm from the object). Then secondary electrons produced on the MCP entrance are amplified in its pores. Once amplified electrons exit the MCP, they are accelerated by phosphor potential (to 3~6 kV) and converted to optical light on a phosphor. The optical signal from the phosphor is transferred to a recording device (charge-coupled-device (CCD) or a photographic film) by a fiber-optic plate (FOP)[1].

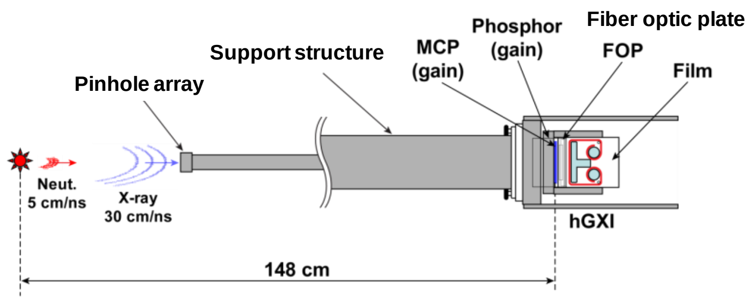

Fig. 1. Typical setup of an x-ray framing camera for gated pinhole x-ray imaging. The MCP gain is turned off on arrival of 14 MeV neutrons. However time integrating components following the MCP (phosphor, FOP, and photographic film) remain sensitive at the neutron arrival time.

To avoid image blur due to fast motion of an object, temporal gating of x-ray camera is crucial. The x-ray sensitivity of the camera is switched by supplying high voltage pulse on arrival of x-ray signal (~5ns after the x-ray emission on the object). The 14 MeV neutrons produced in the compressed plasma travels ~5.1 cm/ns and hit the detector ~24 ns after the x-ray arrival. Therefore there is time difference between the x-ray and the neutron arrival. This delay helps to reduce the background because the MCP gain is turned off when neutrons hit the detector. However time-integrating components following the MCP (phosphor, photographic film) are still sensitive to excitation by ionizing radiations induced by neutrons [2-4]. Therefore, the neutron sensitivity of those time integrating components is important.

3. Possible mechanisms of fast neutron induced background

Fig. 2 shows possible mechanisms of neutron induced background on time integrating components of the camera. First, neutron produces various charged particles in the sensitive layer of the photographic film. Protons and other light nuclei recoiled by 14 MeV neutrons deposit energy in the emulsion layer. Because of their longer mean free path, protons produced in the FOP by (n,p) reactions can also reach the sensitive layer and contribute to the background exposure. X-rays induced by those charged particles excite the film also. The 14-MeV neutrons have enough energy to cause nuclear excitation of materials surrounding the film. Gamma-rays produced by (n,n')γ reactions cause Compton scattering around the detector and then high energy knock-on electrons excite the sensitive layer.

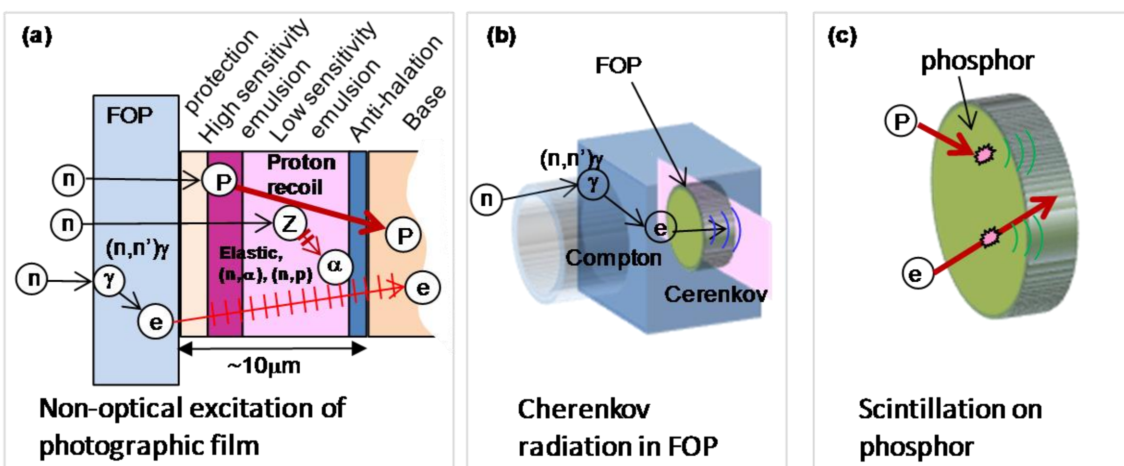

Fig. 2. Possible mechanisms of neutron induced backgrounds on an x-ray framing camera. (a) Non-optical excitation induced by neutron (charged particles and x-ray) directly exposes the sensitive layer of the photographic films. (b) High energy electrons induced by neutron interaction can produce Cherenkov radiation and scintillation in the FOP. (c) Neutron induced secondary charged particles excite phosphor layer.

Second, those high energy electrons cause Cherenkov radiation in the FOP and optically excite the photographic films. Third, the charged particles produced by neutron interaction excite the phosphor layer also.

4. Experiments

To understand the contribution of the different excitation mechanisms, we assembled test camera head with the time integrating components (phosphor, FOP, and photographic film). Figure 3(a) shows exploded view of the test camera head. The film cassette was located 43.2 cm from the OMEGA chamber center.

A photographic film (Kodak TMAX 3200) was set in an aluminium cassette with various samples. Figure 3(b) is showing a film exposure data when neutron flux was 3×10^9 neutrons/cm^2. The optical density of the film was converted to equivalent optical exposure (erg/cm^2) using a sensitometry test sample (a piece of the film which is pre-exposed to known light fluence, and developed simultaneously with the data film).

A part of film which is exposed to all the background mechanisms (non-optical, optical excitation from FOP, and optical excitation from phosphor) showed optical density corresponding to 0.035erg /cm^2. In order to separate optical and non-optical, visible light signal was partially blocked with thin black paint on the FOP surface. As shown in Fig. 3. (c), region under the light block has exposure of 0.019erg/cm^2. Therefore about 50% of the recorded background was non-optical exposure. To differentiate the optical exposure from the phosphor and the FOP, a part of the phosphor coating was removed from the FOP. Difference of exposure with and without phosphor was ~ 0.004 erg/cm^2. Therefore about 40% of the background comes from the FOP and 10% is from the phosphor as optical excitation. A plastic (1mm thick) and a tantalum (0.8mm thick) sample were placed in front of the film to enhance the neutron induced ionizing radiation. As expected, exposure of the region covered with plastic was higher (0.07 erg/cm^2) than the region covered with aluminium (0.018 erg/cm^2). This enhancement is due to energy deposition from recoiled protons. The region covered with the tantalum disc (0.03erg/cm^2) was also higher than the region covered by aluminium because of x-ray fluorescence of tantalum excited by neutron induced charged particles.

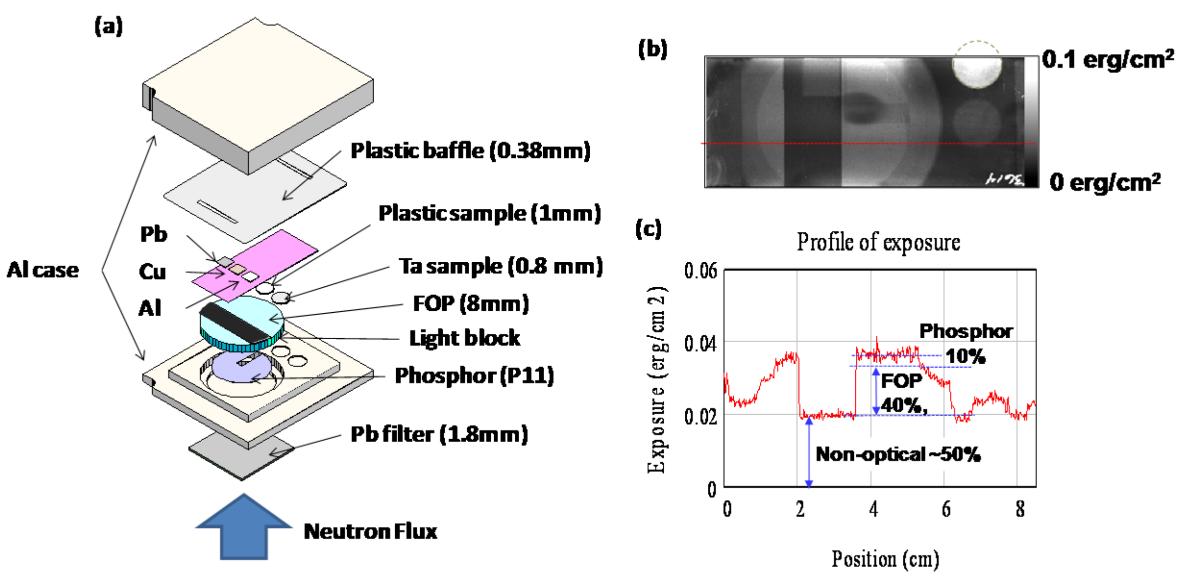

Fig.3. Experimental setup of neutron induced background test; (a) an explode view of the test head, (b) Image observed with TMAX 3200, (c) a line profile of the image through the red line on (b).

In addition, four different materials were attached to the back side of the film; Pb, Cu, Al, and plastic. No significant difference was observed between the plastic (0.02erg/cm^2) and the aluminium backing (0.018 erg/cm^2). This is explained by the direction of the recoiling protons. Since neutrons come predominantly from the center of the target chamber, most of the protons recoil away from the film and cause little exposure. The regions backed by the Cu foil (0.023 erg/cm^2) and the Pb foil (0.028 erg/cm^2) were higher than the aluminium backing due to x-ray fluorescence from those materials.

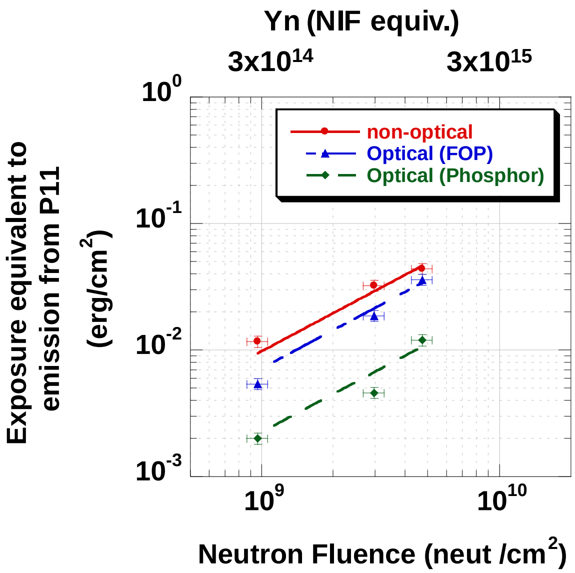

Fig. 4. Observed background exposure versus neutron fluence. The background exposure from each mechanism scales with neutron fluence.

Fig. 4 shows the observed background versus 14 MeV neutron fluence inferred from independent neutron production measurements. Background exposure of each component showed linear dependence on neutron fluence. This confirms that the background exposure was neutron induced.

5. Discussion

Because the background exposure showed good scaling with neutron fluence, it is possible to assess neutron induced background of actual NIF implosion experiments. For a detector-to-target distance of 148 cm and a neutron production yield of 5×10^{14}, (14 MeV neutron fluence ~ 2×10^{9} neutrons/cm^2), the expected background exposure is 0.03erg/cm^2. According to previous work [5], the maximum x-ray signal turns into non-linear region at an output image intensity of 0.2erg/cm^2 when phosphor potential is set to 3 kV. By increasing phosphor potential to 6 kV, the linear response limit of the x-ray signal can be increased to 0.4erg/cm^2. Therefore the expected background exposure of the shot is less than 10% of the maximum x-ray signal.

Acknowledgements

The authors acknowledge the support of the Omega crew, J. Emig, J. Tellinghuisen, S. Evans, V. Rekow, N. Hill, J. Armstrong, G. Pien, S. Alvarez, M. Moran, K. Loughman, S. Dent, S. Lucas, O. Gotchev, and W. Shmayda. Prepared by LLNL under Contract DE-AC52-07NA27344

References

[1] J. D. Kilkenny, Laser and Particle Beams 9, 49 (1991).
[2] R. A. Lerche, Rev. Sci. Instrum. 68, 628 (1997).
[3] P. A. Jaanimagi, R. Boni, and R. L. Keck, Rev. Sci. Instrum. 72, 801 (2001).
[4] J. L. Bourgade, et al., Rev. Sci. Instrum. 75, 4204 (2004).
[5] O. L. Landnen, et al., Proc. SPIE 2002, 2 (1993).